# Implementation of a microchannel manufacturing system based on micro-Electro Discharge Machining

**Oscar Chaídes[1], Horacio Ahuett-Garza[1], Allen Y. Yi[2]**

[1] Department of Mechanical Engineering, Tecnológico de Monterrey, Campus Monterrey
Eugenio Garza Sada 2501, 64849 Monterrey, N.L. México, TEL. +52 (81) 83582000 Ext. 5430;
[2] Department of Integrated Systems Engineering, The Ohio State University
210 Baker Systems Building, 1971 Neil Avenue, Columbus, OH 43210, United States, TEL. +1 (614) 292-9984;
e-Mail: oscar.chaides@exatec.itesm.mx, horacio.ahuett@itesm.mx, yi.71@osu.edu

## Resumen

El presente trabajo presenta un sistema para manufactura en metales conductores utilizando micro maquinado por electro erosión. El sistema está basado en un circuito oscilador resistivo-capacitivo que produce las descargas eléctricas para la remoción de material. El diseño del control propuesto y de la estructura mecánica de la máquina combina las capacidades de electro erosión convencional para penetrar materiales conductores, con un movimiento lateral del electrodo, permitiendo la generación de micro canales. Guías lineales de precisión con motores a pasos fueron empleadas para el posicionamiento de la herramienta de trabajo. Un porta electrodo con capacidad de oscilación fue desarrollado para mejorar el desempeño del sistema. El porta electrodo facilita la expulsión de partículas residuales durante el proceso. El sistema de control computarizado empleado está basado en una distribución libre de Linux específica para control de máquinas herramientas (LinuxCNC). El control de espaciamiento necesario para la continuidad del proceso fue implementado mediante el monitoreo del voltaje electrodo-pieza. Microcanales de 290 μm de ancho, 50 μm de profundidad y decenas de milímetros de largo fueron manufacturados como pruebas de validación en acero A36 (96.9 HRB) utilizando electrodos de latón de 254 μm de diámetro. El control fue utilizado en dos diferentes configuraciones de máquina, probando la portabilidad del diseño propuesto.

## Abstract

This document presents a micromanufacturing system by micro electro discharge machining (μEDM). The system implements a resistor capacitor oscillator (RC oscillator) as a power source for the material removal process. The architecture of the machine allows an operation that combines features of the conventional plunge electrical discharge machining process with a lateral motion of the oscillating electrode to produce micro channels. High precision linear stages actuated by micro stepping motors were used for tool displacement. A mechanical electrode holder, capable of oscillation, was developed to improve both flushing of sediments and the overall material removal rate. Tool motion was controlled using an open source machine control, LinuxCNC. The gap control methodology for process continuity was implemented using a gap monitor based on the voltage difference between the electrode and the working piece. The system was used to manufacture microchannels of 290 μm width, 50 μm depth and several millimeters long in A36 steel (96.9 HRB) using a brass electrode with a 254 μm diameter. The control system was used in two different machine configurations, thus proving the portability of the proposed design.

**Palabras clave:**
Micromaquinado, Linux, electroerosión, cabezal oscilador.

**Keywords:**
Micromachining, oscillating tool holder, Linux, electric discharge machining

## Notation

| | |
|---|---|
| *μEDM* | Micro-Electro Discharge Machining |
| *CAD* | Computer Aided Design |
| *CNC* | Computer Numerical Control |
| *LinuxCNC* | Open source CNC controller |
| *PZT* | Lead zirconium titanate |
| *RC* | Resistive-Capacitive |

## Introduction

There is an increasing demand for high precision, miniaturized components, in fields that range from consumer products to biomedical equipment. To meet quality and throughput demands for these products, new manufacturing process that offer reduced size and energy consumption are being developed [1].

Different processes, such as photolithography, microgrinding and micromachining, are capable of producing geometric features in the micro-meso scale [2, 3] (anywhere

between 1µm to a few mm). These processes can be used to manufacture general purpose microparts in various materials such as ceramics and metals. However, recent trends require the design, manufacture and testing of sophisticated components such as micro-chemical units and micro-molds for plastic injection [4]. Although geometric features for these parts or their molds can be produced by the previously mentioned processes, micro electrical discharge machining (µEDM) presents an interesting alternative because of its capacity to work with hard conductive materials.

The µEDM process can be used in parts that require high precision and a fine surface finish. Manufacture of small holes of a few micrometers of diameter is one of the most extended applications of µEDM [5]. µEDM can be used in conjunction with electro chemical machining to achieve excellent surface roughnesses, of less than 1 µm Ra [6]. µEDM has also been used for the manufacture of micro features in stainless steel [7], a material that is particularly challenging for conventional machining. Due to the high cutting speeds involved, conventional micromachining processes rely on diamond tools. However, diamond tools are not used for steel machining because of their chemical affinity. As a consequence, aluminum is the material of choice to produce components such as micromolds for plastic injection molding [8]. µEDM offers the potential to use stainless steels and other high strength components for micromold fabrication, allowing more aggressive parameters for injection molding. Micro-chemical units, i.e. micro mixers and micro reactors designed to improve the efficiency of chemical production, are a typical application of stainless steel parts machined by µEDM [9]. µEDM can be used to fabricate microchannels in steel or other high strength materials, which are needed to withstand the high temperatures and high pressures that take place during the reactions in micro-chemical units [10]. The main advantage of µEDM over other conventional micromanufacturing process is its ability to machine hard conductive materials without the use of expensive tools. In particular, µEDM can process materials whose hardness exceed 40 HRC, and is also capable of generating geometric features with aspect ratios higher than 6 [11]. Other important characteristics of µEDM are the relatively slow velocities involved, and the lack of physical contact between tool and workpiece [12]. As a consequence, the positioning system is not subject to forces from the material removal process. In particular, previous research has shown that stepper motors can be used in precision positioning if the correct control technique is employed [13,14], reducing overall cost for a precision system.

Different challenges exist for EDM when applied to micromanufacturing. A critical requirement to maintain a constant depth of cut is that the position of the electrode in the vertical direction needs to be regulated to compensate for electrode wear. Without this compensation, the process cannot be used to produce complex geometries, i.e., only holes could be machined. The design of a controller to compensate for the electrode wear is difficult because of the no-linear and time-varying characteristics of the process [15]. Discharges between the full surfaces of the electrode and workpiece occur when the voltage becomes large enough to overcome the dielectric strength of the dielectric fluid. Discharges occur randomly, making it difficult to accurately predict the geometric characteristics of the finished part. Discharge control is critical for such an accuracy of the process.

This article presents the construction of a µEDM machine and describes the design and implementation of its control system. The system uses a resistor capacitor (RC) oscillator for the material removal process. To improve flushing of sediments and removal rate of material, an electrode holder capable of oscillation was developed. The motion displacement of the tool was controlled using the open source machine control LinuxCNC. The gap control methodology for process continuity was implemented using the open electronics platform Arduino. A gap monitor based on voltage difference between electrode and workpiece was developed using operational amplifiers. The particularity of the proposed control system is that it can be used to produce microchannels. The architecture of the machine allows for an operation that combines features of the conventional plunge µEDM process, with a lateral motion of the oscillating electrode. High precision linear stages actuated by micro stepping motors were used for tool displacement.

**µEDM process characteristics**

The µEDM process uses instantaneous discharges of energy from an electrode to remove material from a workpiece [16]. The removal mechanism is based on the generation of a plasma channel that vaporizes a small fraction of material. This process produces micro-craters in the workpiece and the loss of material of the electrode. During operation, the workpiece is submerged in a dielectric fluid, which helps with the removal of the debris and cools down the work area. The energy consumed in each discharge is of the order of $1 \times 10^{-5}$ J. For the process to be continuous, the electrode and part need to be separated by a relatively constant distance, or gap, of a few micrometers. Two types of power sources exist that are capable of producing the required sparks. The first one is based on an RC oscillator with a discharge frequency determined by its own time constant. The second one uses switching electronics. When the first method is chosen, gap size monitoring and control become critical factors due the fact that the process continuity relies on constant and controlled spacing. With voltage differences lower that 100Vdc between workpiece and electrode, a gap of around 7 µm can lead to a continuous and stable process for microhole fabrication [17].

The µEDM process is considered stochastic and different techniques have being used to control it, for example, Neuronal Networks [xx]. In general, direct measurement of the gap is very difficult. Consequently, indirect methods to estimate its size have been developed.

The method used in this work is based on the sensing of the voltage between electrode and workpiece. This method interprets the voltage difference as a representation of the magnitude of the gap [19]. In particular, the technique proposed in this work is based on pre-defined voltage levels. This concept is explained in the following sections.

**Machine and control architecture**

The system presented in this work was designed to produce microchannels by the μEDM process. The machine architecture consists of three different subsystems, shown in Figure 1: Mechanical Systems, Electronics, and the Software Module. The elements the make up each one of these elements are summarized in the figure. Each subsystem constitutes a module that interacts with the other modules to perform the μEDM process.
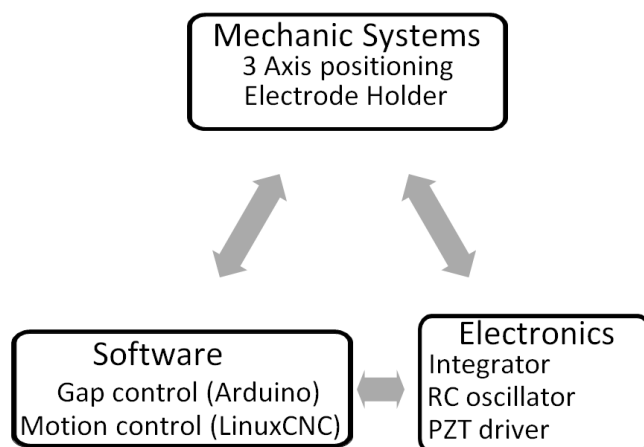


```
┌─────────────────────────┐
│   Mechanic Systems      │
│   3 Axis positioning    │
│   Electrode Holder      │
└─────────────────────────┘

┌──────────────────────┐      ┌──────────────────┐
│     Software         │      │   Electronics    │
│ Gap control (Arduino)│◄────►│   Integrator     │
│ Motion control       │      │   RC oscillator  │
│   (LinuxCNC)         │      │   PZT driver     │
└──────────────────────┘      └──────────────────┘
```

**Fig 1**. Micro EDM machine architecture and subsystems.

The synchronization of the different subsystems is done with the use of signals. These signals are not homogenous and vary in amplitude, frequency, and meaning. Figure 2 shows the interconnections between subsystems and the signals used for synchronization.

Four different types of signals are presented in the figure. The first are binary signals, defined between 0 and 5 VDC and used in pulsing trains of increasing or decreasing values for enabling and disabling features of the system. The second type corresponds to analog signals, for example sine voltage waves, used to produce oscillation by the PZT or generate a voltage between the electrode and workpiece. These signals vary in time and amplitude depending on the needs of the subsystems using them. The third type involves data exchange between software and hardware, managed internally by the host PC that controls the system. The fourth type deals with mechanical motion or displacement produced by the PZT and the linear axis. The different modules and their interactions are discussed in the next sections.

**Mechanical structure**

The mechanical components of the system are shown in Figure 3. The basic system was constructed based on a commercial CNC minimill from Sherline (8540 metric) with the following capabilities; "Y" travel = 127 mm, "X" travel range = 228 mm, "Z" travel range = 159 mm. The maximum travel speed of this machine is 558.8 mm/min. A maximum backlash of 0.076 mm in each axis is standard for this machine. The hardware of the machine was modified slightly to accommodate the process. In particular, the spindle was removed and replaced by an electrode holder. Similar minimills have been used for micromanufacturing due to their
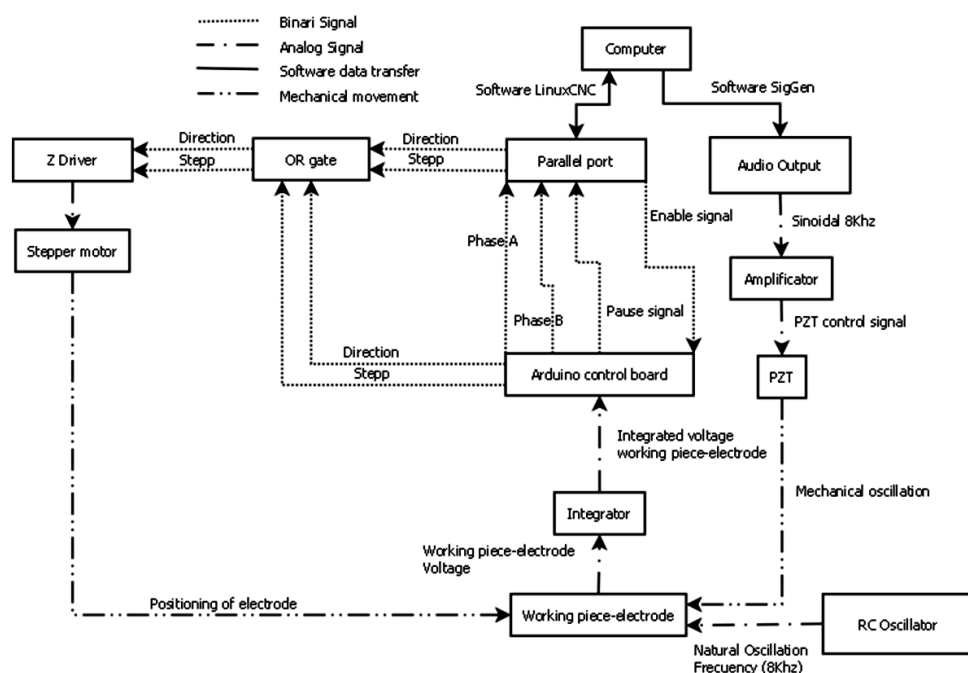


**Fig 2**. Signals and interconnections used for synchronization of the different functions of Microchannel μEDM machine.

availability and low cost [20]. An acrylic thank with a work-piece holder was incorporated to the minimill. Automotive synthetic oil was employed as dielectric fluid in the process tank.

Standard Sherline machines are equipped with a LinuxCNC motion controller. To reduce costs, the parallel port of a computer was used as interface to communicate the computer controller with the stepper drivers. This open source motion controller gives the user access to internal flags that can be used to modify the behavior of the controller. Motion of the milling machine was programmed in standard G code (RS-247). The control system was adapted to account for the gap compensation needed in the EDM process. In particular, the Z axis motion control was modified to allow retraction of the electrode when the gap is too small, without losing track of the position of the axis when a retraction is ordered.
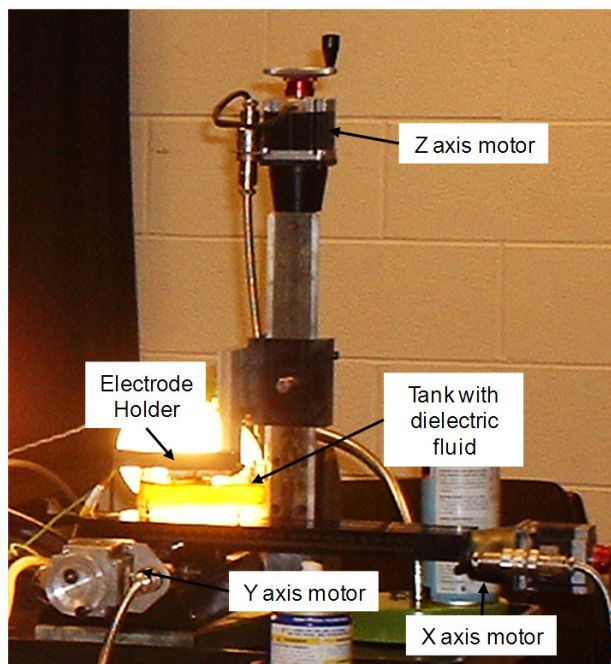


**Fig 3**. Modified minimill with mechanical elements of the μEDM system.

The machine uses stepper motor size NEMA 23 of 1.8° per step. A 1/5 microstepping driver was used to increase the re-

solution of displacement of each axis. The screw lead was 1 mm, producing a theoretical resolution of the axis of 1 μm micrometer. In practice it is not possible to achieve the theoretical resolution because of friction, backlash and accumulated error in the screw thread. The backlash of the axis was reduced to a minimum of 70 μm. The motion control software can compensate for this backlash to improve precision.

The electrode holder assembly was designed to produce oscillation of the electrode at the same frequency that the RC oscillator produces sparks (8 KHz). The small mass of the electrode allows for mechanical displacement with relatively small energy consumption. As explained before, the electrode oscillation helps remove debris from the discharge region. Figure 4 shows a schematic of how the electrode retraction also helps remove chips and excess material from the work zone.

A PZT bimorph was used to produce oscillation of the electrode. During the EDM process, the PZT bimorph is excited with a sinusoidal signal amplified by a commercial audio amplifier. This excitation produces displacement of the bimorph with a magnitude required for spark production (about 7 microns). An electrode holder is attached to the center of the circular bimorph. The electrode holder consists of a plastic cylindrical part that permits the electrical contact of the electrode with the RC oscillation circuit. The holder has a hole where the electrode is inserted. Commercial brass wire for Wire-EDM of 254 μm of diameter (Hitachi HBZ-K Cu60 Zn40) was used as an electrode. Figure 5 presents the electrode holder and the bracket design for attachment to the Z axis of the minimill.

**Electronic Module**

The electrode oscillation subsystem needed for chip removal requires an excitation signal for the PZT bimorph. The excitation signal is produced by the open source software SigGen in the control computer. A Sinusoidal signal of 1Vp-p of amplitude and 8 KHz frequency was used in the process. This signal was obtained from the audio output of the computer. This audio amplifier was used to amplify the power of the signal and drive the PZT bimorph. Tests showed that
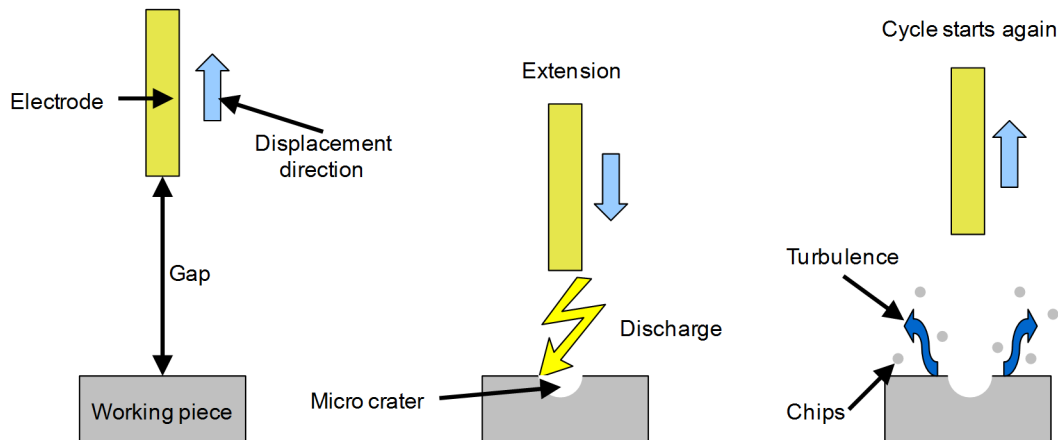


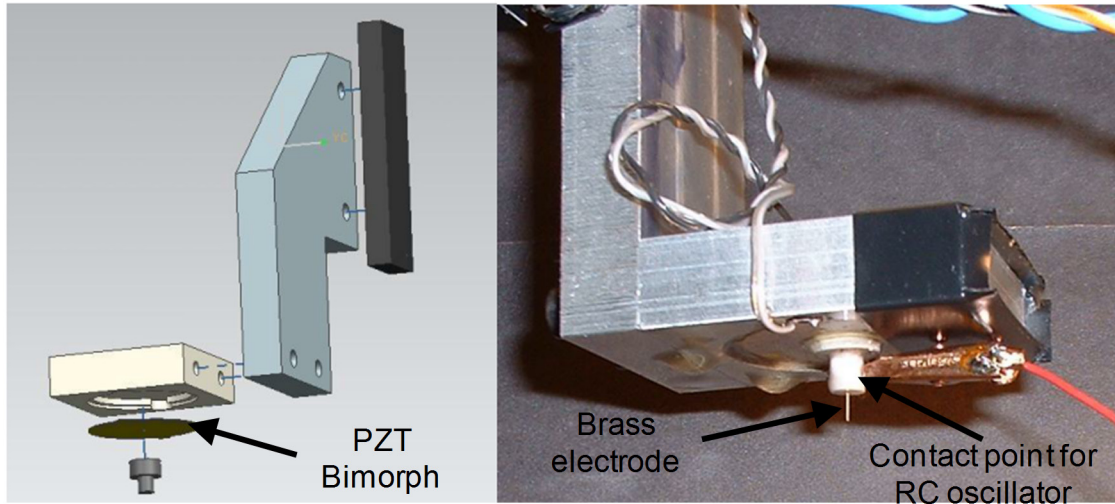**Fig 4**. Electrode oscillation for chip removal.

**Fig 5**. Electrode holder, a) CAD model. b) Assembly.

the bimorph was not capable of producing displacement of the required magnitude at higher frequencies. Basically, for a given frequency the power consumption of the bimorph beyond certain amplitude increased until the PZT was destroyed by thermal effects. As explained before, the frequency of oscillation was tuned to the RC oscillator frequency of the spark generator power supply. By design, it was expected that for each cycle of retraction and advance of the oscillating electrode holder, a single spark would be produced to remove material.

The maximum oscillation frequency of the bimorph constituted a limitation of the design that influenced the choice of the capacitor and resistor for the RC oscillator circuit. Tests showed that a 98% charge is needed in the capacitor for the production of a spark capable of producing a microcrater in the workpiece. Equations 1 and 2 were derived from the basic equations of energy storage in a capacitor and RC resonant circuits. The energy per discharge required for the process reached 100 µJ, while a voltage of 60 V was required between electrode and workpiece. This requires a capacitance of 0.056 µF and a resistance of 563 Ohm.

$$C = \frac{2 * E}{V^2} \tag{1}$$

$$R = \frac{t}{4 * C} \tag{2}$$

The voltage difference between electrode and workpiece was used as an indirect measure of the gap size, and is referred to as "gap voltage". As explained before, in normal operation, discharges are produced at a rate of 8 KHz. If the electrode is farther from the workpiece than the distance needed for discharge, and open circuit voltage will be reported. In the opposite condition, if the electrode is touching the workpiece a zero voltage will be reported. Integration over time of the gap voltage is used for gap control. Equation 3 was used to calculate an average gap value [21]. This value was then used as input by the microcontroller for gap control and was com-

puted in an analogical way to speed up the process.

$$Vgap = \int \frac{-Vin}{RC} \, dt \tag{3}$$

The actual gap voltage (60 Vdc) was reduced below 5Vdc by a current divider resistor, to be compatible with the ADC capabilities of the Arduino UNO board. The integrator was implemented in an electronics circuit based on operational amplifiers. A voltage follower, a low-pass filter and a voltage inverter were used in sequence to obtain the desired behavior. Figure 6 shows the schematic of the integrator. The low-pass cut frequency was set to 80Hz and the RC oscillation frequency was a hundred times larger, resulting in the integration of the signal. Figure 7 shows the results of a comparison of the gap voltage before and after the integration.
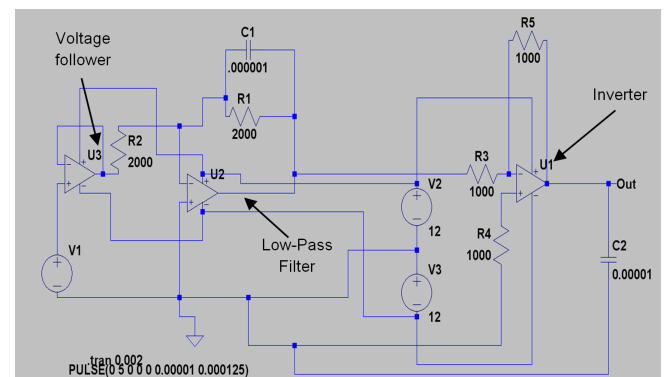


**Fig 6**. Integrator diagram for gap control.

An integrated voltage signal showing small slope, indicates a better control of the gap distance and a better control of the spark generation for the µEDM process.

**Software Module characteristics**

Commercial µEDM machines are controlled by special software designed specifically for the process. In general, conventional control software for CNC machines are not capa-

ble of retraction of the axis for the purposes of gap control. However, LinuxCNC can be modified by the user to fit the needs of the process, which made it suitable for the purposes of this work. The parallel port of a computer was used for the interaction of LinuxCNC with the different modules of the machine (see Figure 2). The signals for step and direction of each axis were taken from this port.
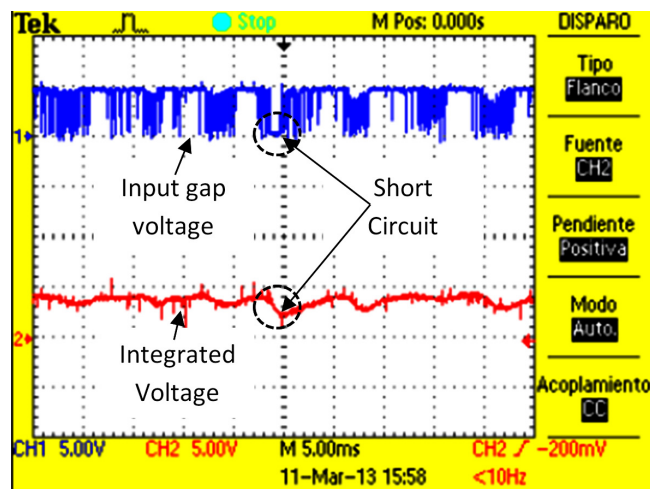


**Fig 7**. Gap voltage signal before (blue signal) and after integration (red line).

LinuxCNC includes a sub library called HALUI that enables the use of binary signals to control the behavior of the controller and allows the connection of external subsystems as well as extend functionality. These features make LinuxCNC extremely flexible and adaptable. As input, LinuxCNC reads a series of G and M codes for machining. These codes are generic for CNC controllers. The program used by LinuxC-NC does not contain information about the gap or the µEDM process, and it is executed by the controller in the same way it executes all other non-specific programs. The gap control decisions are taken by the Arduino UNO board. To communicate with the LinuxCNC host PC, the Arduino Board uses 4 binary signals that are transmitted over the parallel port. Table 1 summarizes the signals and their meanings.

When the Enable signal is TRUE, the Arduino UNO board continually reads the integrated gap voltage value using one analog channel. Voltage data is collected every 100 milliseconds. Depending on the current gap voltage, the Arduino UNO board takes actions to maintain a constant gap size. Four gap voltage zones were defined, as described in Figure 8.

If the gap voltage lies between 100% (60 Vdc) and 90% (54 Vdc) of the nominal gap voltage (60 Vdc), the voltage is considered to be in Zone 1. A gap voltage in Zone 1 indicates that the distance of the electrode to the workpiece is too large and non-discharge conditions are taking place. Under these conditions the speed of displacement of the codes interpreted by LinuxC-NC is increased by 10% each 100 milliseconds, until a maximum of 150% of the feed speed programmed in the G code is reached. If the gap voltage lies between 90% (54Vdc) and 50% (30Vdc) of the nominal gap voltage, the voltage is considered to be in Zone 2. In this zone, the execution of displacement com-

mands programmed in LinuxCNC continues without change at a constant speed. If the gap voltage lies between 50% (30Vdc) and 10% (6Vdc) of the nominal gap voltage, the voltage is considered to be at Zone 3. In this zone the speed of displacement of the codes interpreted by LinuxCNC is decreased by 10% each 100 Milliseconds, until a minimum of 10% of the feed speed is reached. If the gap voltage drops below 10% (6Vdc) of the nominal gap voltage, the voltage is considered to be in Zone 4. Voltage in this zone indicates that a short circuit between electrode and workpiece is imminent or that it is already happening and an immediate retraction of the Z axis is needed to break it. In Zone 4 the Arduino UNO board sends a signal to the LinuxCNC interpreter to pause all movement of the electrode. The Arduino UNO board takes control of the Z axis using an OR gate and starts retraction of the Z axis one step every 100 milliseconds. After each retraction step the gap voltage is monitored. If the gap voltage returns to nominal values, it is assumed that the short circuit has been eliminated and the electrode is returned to its original position, that is, at the instant that the short circuit condition was encountered. At this time, the pause command is removed by the Arduino UNO board and displacement of the electrode continues to be controlled by LinuxCNC.

**Table 1**. Signals for gap control between LinuxCNC host computer and Arduino UNO Board.

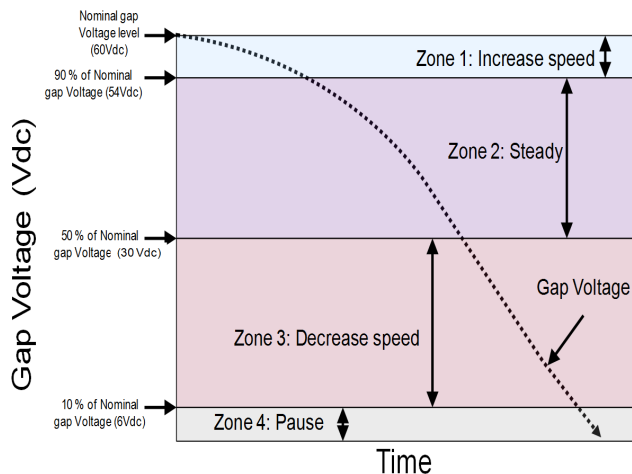| Name | Source | Destination | Function |
|---|---|---|---|
| Enable | LinuxCNC host computer | Arduino UNO board | This signal enables the gap control. A logical 0 indicates that the CNC controller is in standby and a logical 1 indicates that gap compensation is required. The S command in the LinuxCNC controller replaces the start of the tool rotation by a gap compensation motion. |
| Pause | Arduino UNO board | LinuxCNC host computer | This signal indicates that a low gap voltage has been detected and the gap needs to be restored. The execution of the CNC instructions is paused placing the feed speed to 0 until gap voltage is restored to normality. Encoder Phase A |
| Encoder Phase B | Arduino UNO board | LinuxCNC host computer | These two signals are used to emulate the presence of an encoder wheel with quadrature for feed control of the programmed movements. If the gap voltage is dropping, the speed of the controller is reduced. If the voltage is rising, the speed is increased. |

**Fig 8**. Gap voltage zones specified for gap control.

The binary signals generated by the Arduino board are manipulated by software using the Hardware abstraction layer (HALUI) of LinuxCNC. The control of speed and holding of movements that depend on the gap voltage zones was done using two internal signals:

- motion.feed-hold: this is a binary signal that stops motion ordered by the controller.
- halui.feed-override.counts: This signal is connected to a quadrature virtual encoder simulated by the Arduino UNO board, and controls the percentage of feed speed of the current displacement of the electrode ordered by the controller.

**Results: µEDM machine performance**

For the testing of the system capabilities, different geometries were manufactured in a cold worked A36 steel rectangular workpiece. The rectangular slab dimensions were 0.03 m X 0.015 m X 0.01 m and had a hardness of 96.9 HRB. The upper face of the workpiece was polished to a mirror finish (Ra = 0.1 µm) to provide a reference surface for optical measurements. Micro holes were fabricated on this surface, with a separation of 1 mm between successive holes. Direct polarity (Positive terminal on the electrode and negative on the workpiece) was used for the test. The program called for a hole of 0.1 mm in depth to be machined, with a feed rate of 0.08 mm/sec, starting from the point where the electrode was in contact with the surface of the workpiece (G01Z-0.1F0.08S1).

An optical profilometer and microscope were used to analyze the finished holes. The roughness, depth and time to fi-

nish the holes as well as the initial and final electrode lengths were registered for each test. The material removal rate and electrode-piece wear rate were calculated with this data. Figure 9 presents one of the machined microholes, where a radial overcut of 18µm produced by the lateral discharges of the electrode of 254 µm of diameter can be observed.
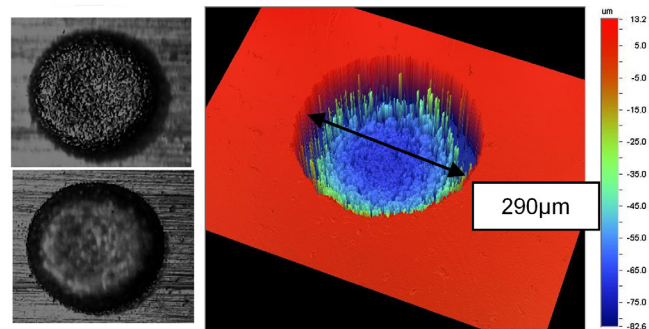


**Fig 9**. Microholes produced in steel. Optical image and 3D representation reported by the profilometer.

The data collected from three consecutive tests is shown in Table 2. The average material removal rate was calculated to be 0.0231 mm3/min, with a roughness Ra of 0.62 µm, electrode wear ratio of 0.47 µm/µm and depth of 76.5 µm.

As seen in the table, on average, the actual depth that was reached amounts to about 76.5% of the programmed depth. The difference was caused by the electrode wear. With this information, new tests were conducted for a specified depth of 50 µm. In these cases, the program ordered the controller to reach a depth of 0.065 mm at the same feed rate (G01Z-0.065F0.08S1). Six holes were produced for these conditions. The average depth of these microholes was measured at 50.59 µm, which represents a deviation from the expected depth of 1.18%.

In a different capability test, a channel was produced. With the electrode at the desired depth of 50 µm a lateral displacement command was given to the motion controller in the X axis direction. The resulting channel is shown in Figure 10. As can be seen, the depth of the channel is not constant. The lateral motion of the electrode produced further wear, leading to a variation of channel depth. The slope of the bottom of this channel reached an angle of 4.123° in the direction of cut (along the channel). This angle was considered for further compensation of the electrode wear. As an example, a lateral displacement of 1 mm requires a compensation of 0.072 mm in the Z negative direction

**Table 2**. Data from microhole machining test.

| Test No. | Electrode Initial length (mm) | Electrode Final length (mm) | Electrode wear (mm) | Deep (mm) | Electrode wear ratio (um/um) | Time | Material removal rate (mm3/min) | Ra(mm) |
|---|---|---|---|---|---|---|---|---|
| 1 | 6.9 | 6,86 | 0.04 | 75.3 | 0.531 | 9.6 | 0.024 | 0.48 |
| 2 | 6.49 | 6.46 | 0.03 | 75.3 | 0.398 | 9.8 | 0.023 | 0.83 |
| 3 | 6.7 | 6.66 | 0.04 | 78.9 | 0.507 | 10.8 | 0.022 | 8.57 |

to accommodate for electrode wear (digging further into the part). The resulting motion command for a 1 mm channel machining starting from a depth of 50 µm was G01Z-0.072X1F1S1. This motion compensated for electrode wear and was intended to maintain the channel depth for every mm of longitudinal travel.
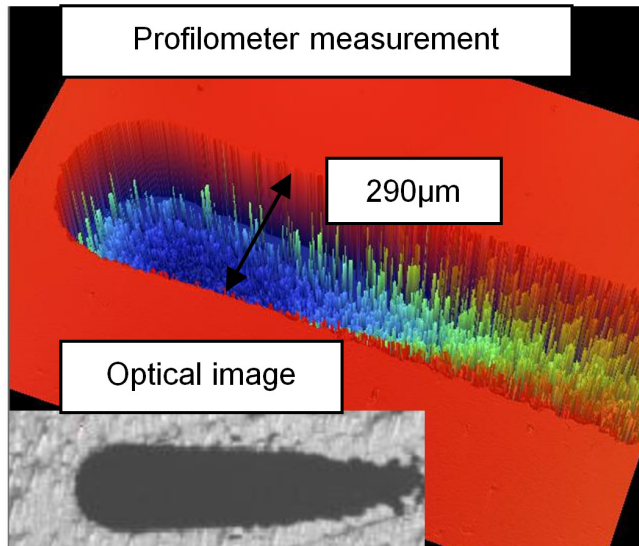


**Fig 10**. 50µm deep microchanel showing slope caused by electrode wear.

This compensation technique was used for the fabrication of microchaneels on A36 steel. The depth of the channels for this study was designed to be 50 µm. Microchannels with changing direction of 90° were chosen to test the capability of the mechanical and controller backlash compensation. The controller was programmed to do a small pause before changing direction using a common machine tool approach called exact stop mode, programmed with the command G61.1. The resulting channels are show in Figure 11. As can be seen, the channel width exceeds the electrode diameter by about 36 µm. Depth of the channel was fairly constant, at the intended 50 µm.

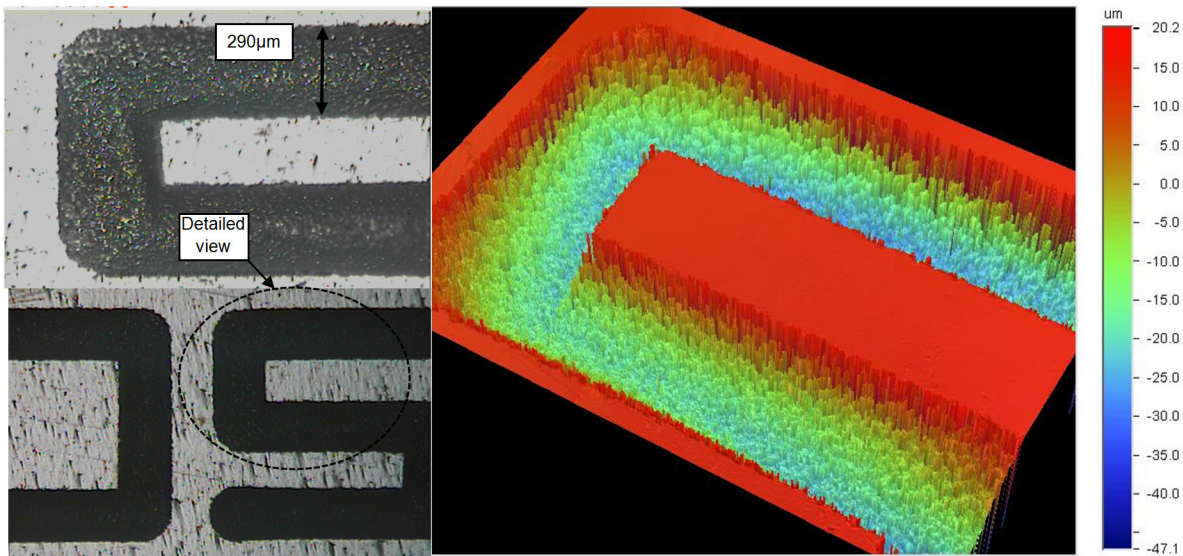## System Portability

In order to prove the portability of the proposed control system, a different mechanical architecture was developed. An orthogonal array of three axis in a Gantry configuration was used. Each axis consisted on a commercial linear microstage with preload and free of backlash. The linear stages are equipped with 1.8° steppers and 1/10 microstepping drivers. Figure 12 shows the mechanical assembly. The same electrode holder and fluid thank were used.
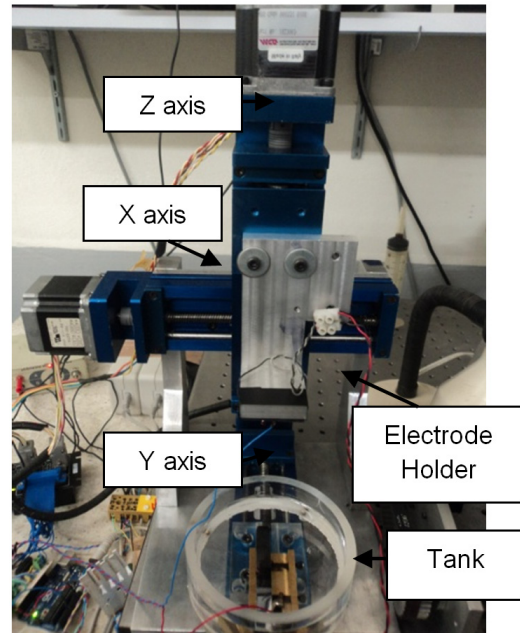


**Fig 12**. Gantry configuration for control system portability test.

This machine was slightly more accurate than the Sherline, and therefore it was possible to experiment with other channel geometries. Figure 13 show a spiral microchannel fabricated with the gantry configuration. The same electrode wear compensation technique was used to obtain a constant depth of 50 µm.
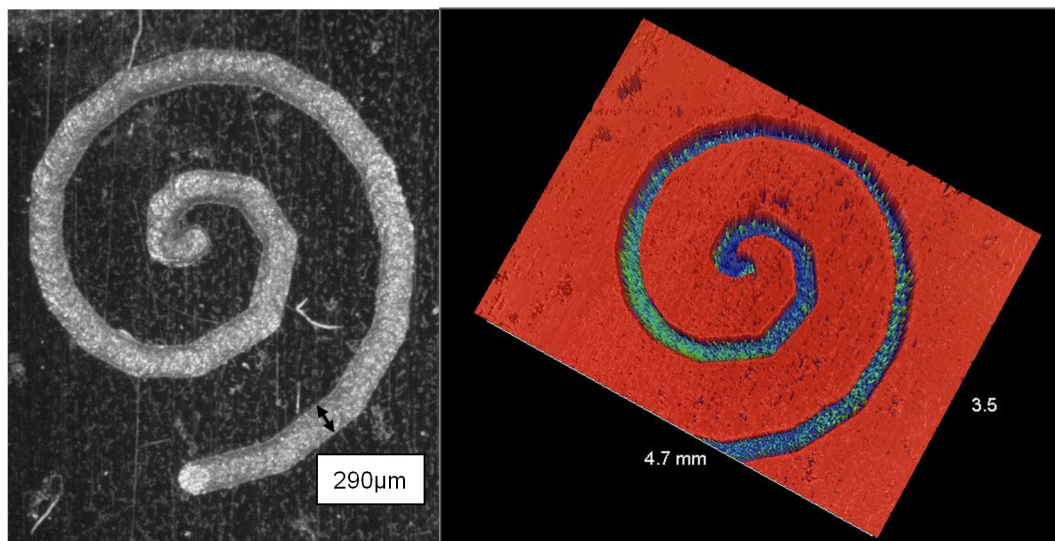


**Fig 11**. Microchanels: optical and profilometer 3D image.

**Fig 13**. Machined spiral microchannels in gantry mechanical setup. Optical image and profilometer measurement.

These tests showed the capabilities of the control in 3 axis, simultaneously. The commands used for the spiral microchannel were a sequence of lineal displacement of small longitude interconnected in the XY plane. The compensation on the Z axis was calculated for each segment of the spiral and added to the commands to produce the desired channel depth.

## Discussion

The system presented in this work proved capable of performing a µEDM process to manufacture geometric features that measure as little as 50 µm. From this perspective, the architecture of the system met the intended design goals. To achieve these dimensions, trial tests were made and compensation for tool wear had to be programmed.

Given that the exploratory tests were conducted in A36 steel values of voltage and energy used for discharge are not necessarily the same for other materials. Further experimentation is needed for the application of the system in different materials. The magnitude of the electrode wear compensation is affected by the depth of the desired channel. It is conceivable that if the channel's depth changes, the angle of compensation will be altered too. In addition, the tip of the electrode becomes spherical as the process takes place. To produce flat surfaces, more than one machining pass may be required. Multiple passes can also help improve the surface finish of the channel. The surface roughness produced by µEDM is directly related with the energy per discharge developed during the process. For a fast removal of material during a roughing pass, a high level of energy can be used. A finishing pass at low energies will produce better surface finish.

The use of more precise linear axis in the Gantry machine improved the quality of the resulting geometries and allowed micromachining of complex geometries like spirals. Nevertheless, the mechanical construction of both minimill prototypes presented some limitations. In particular, their mechanical characteristics were not designed for micrometric machining. Furthermore, due to the design of the tool holder and PZT actuator, to maintain accuracy a maximum length of 5 mm electrode can be used with the current electrode holder design. As a consequence, channels length was limited to about 10 mm. Finally, as explained in the article, the RC oscillator frequency proposed for this work was limited by the PZT bimorph maximum allowable frequency (8 KHz). A higher RC oscillator frequency can help increase the material removal rate even with the use of lower energy discharges, thus improving quality of the finished product. An improved holder that addresses these issues needs to be designed.

## Conclusions

A new system capable of microchannel manufacturing by µEDM was presented. The proposed system uses low cost hardware and open source software. The employed software can be modified by the user to fit different hardware systems. An electrode wear compensation technique was used to overcome the electrode loss during machining. The system was capable of micromachining A36 Steel with 96.9 HRB, using a brass electrode. The system can be programmed with standard G codes, such as those used in conventional CNC machines.

Our tests confirmed that the architecture of the µEDM machine proposed in this work is capable of delivering a stable process. The machine was capable of producing channels in hardened steel. In particular, shapes such as spirals, which are difficult to produce by conventional means such as machining, were handled without difficulty by the µEDM process. Finally, the portability of the control system was also tested. If required, the positioning hardware can be modified and the control system can be implemented with not special modifications.

While a stable process was delivered by the proposed µEDM machine architecture, it should be pointed out that the experiments shown here were limited in scope. Before introduction to an industrial environment, more tests with different geometries and materials need to be performed. The final goal would be to establish process parameters and tool com-

pensation factors for a wider variety of conditions. Future work will focus on the generation of this data.

As a final note, the structural design of the machine can be improved by enhancing the electrode holder capabilities, in such a way that longer electrodes can be mounted on the machine. Such a modification would allow the fabrication of longer channels for each electrode set up. Current work is underway to produce a new version of the µEDM machine with an improved tool holder.

## Acknowledgements

## References

[1]     Huerta, L. R., Ruiz, A. C., Garza, H. A., García, P., Flores, A., & Kussul, E. "*Diseño de una Micromáquina Herramienta de EDM*". 8º Congreso Iberoamericano de Ingeniería Mecánica. Cusco. Federación Iberoamericana de Ingeniería Mecánica. 2007.

[2]     Kussul, E., Baidyk, T., Ruiz, L., Caballero, A., Velasco, G. "*Development of low-cost microequipment*". Symposium on Micromechatronics and Human Science, IEEE, Nagoya, Japan, pp 125–134, 2002.

[3]     Jauregui A. L., Siller H.R., Rodríguez C.A., Elias-Zuniga A., "*Evaluation of micromechanical manufacturing processes for microfluidic devices*". Int J Adv Manuf Tech. Volume 48, pp 963-972, 2009.

[4]     Giboz J, Copponnex T, Mele P. "*Microinjection molding of thermoplastic polymers: a review*". J Micromech Microeng. 17(6), pp 96-109, 2007.

[5]     Fenske G., Woodford J., Wang J., El-Hannouny E., Schaefer R., Hamady F.. "*Fabrication and Characterization of Micro-Orifices for Diesel Fuel Injectors*", SAE International Journal of Fuels and Lubricants, vol. 1 no. 1, pp 910-919, 2009.

[6]     Zeng Z., Wang Y., Wang Z., Shan D., He X. "*A study of µEDM and micro-ECM combined milling for 3D metallic micro-structures*", Precision Engineering, Volume 36, Issue 3, pp 500-509, 2012.

[7]     Liu K., Lauwers B., Reynaerts D., "*Process capabilities of Micro-EDM and its applications*", The International Journal of Advanced Manufacturing Technology, Volume 47, Issue 1-4, pp 11-19, 2010.

[8]     Yang C., Huang H., Castro J.M., Yi A,Y. "*Replication characterization in injection molding of microfeatures with high aspect ratio: Influence of layout and shape factor*". Polymer Engineering & Science, Volume 51, Issue 5, pp 959–968, 2011.

[9]     Montesinos-Castellanos, A. Thiermann, R., Müller, W., Metzke, D., Löb, P., Hessel, V. & Maskos, M. "*Size controlled polymersomes by continuous self-assembly in micromixers*". Polymer, 53(11), pp 2205-2210. 2012.

[10]     Li, L., Lee, L. J., Castro, J. M., Yi, A. Y., "*Improving Mixing Efficiency of a Polymer Micromixer by Use of a Plastic Shim Divider*". J. Micromech. Microeng. 20, 035012. 2010.

[11]     González V. L. H., Siller, H. R., Rodríguez, C.A., Hendrichs, N.J. "*Caracterización de rugosidad en fresado de alta velocidad de moldes / matrices*". Conference Memories, XVIII SOMIM International Conference, Gto. México 2012

[12]     Morgan C. J., Vallance R. Ryan, Marsh E. R., "*Micromachining glass with polycrystalline diamond tools shaped by micro electro discharge machining*", Journal of Micromechanics and Microengineering, vol 14, pp 1687–1692, 2004.

[13]     Baluta G. y Coteata M. "*Precision microstepping system for bipolar stepper motor control*", in Conference Proceedings of the International Aegean Conference on Electrical Machines and Power Electronics, Muğla, Turkey, pp 291-296. 2007.

[14]     Kussul, E., Huerta, L. R., Ruiz, A. C., Kasatkin, A., Kasatkina, L., Baidyk, T. and Velasco G. "*CNC Machine tools for low cost micro devices manufacturing*". Journal of Applied Research and Technology , Vol. 2, pp 76-91. 2004.

[15]     Chang, Y., Chiu Z., "*Electrode wear-compensation of electric discharge scanning process using a robust gap-control*", Mechatronics, Volume 14, Issue 10, pp 1121-1139, 2004.

[16]     Abbas, N. M., Solomon, D. G., & Bahari, M. F. "*A review on current research trends in electrical discharge machining (EDM)*". International Journal of Machine Tools & Manufacture , Vol. 47, pp. 1214-1228. 2007.

[17]     Chaides O., Ahuett-Garza H., Flores A., Caballero A., Ruiz L. "*Diseño y prueba de un sistema de control de espaciamiento y potencia para Micro EDM*", Ingeniería Mecánica, Tecnología y Desarrollo, Mexico. pp 37-45, 2009.

[18]     Debabrata Mandal, Surjya K. Pal, Partha Saha, "*Modeling of electrical discharge machining process using back propagation neural network and multi-objective optimization using non-dominating sorting genetic algorithm-II*", Journal of Materials Processing Technology, Volume 186, Issues 1–3, pp 154-162, 2007.

[19]     Casanueva R., Azcondo F. J., Bracho S., "*Series–parallel resonant converter for an EDM power supply*", Journal of Materials Processing Technology, Volume 149, Issues 1–3, Pages 172-177, 2004.

[20]     Sodemann, A. A. "*A study on productivity enhancement in high-speed, high-precision micromilling processes*. PhD Thesis*", Atlanta, Ga. Georgia Institute of Technology, 2009.

[21]     Zamora, A. "*Diseño e implementación de una fuente de voltaje con aplicación a micromanufactura por electroerosión*". Tésis de Maestría en Ingeniería. Escuela de Ingeniería, UNAM. Noviembre 2009.